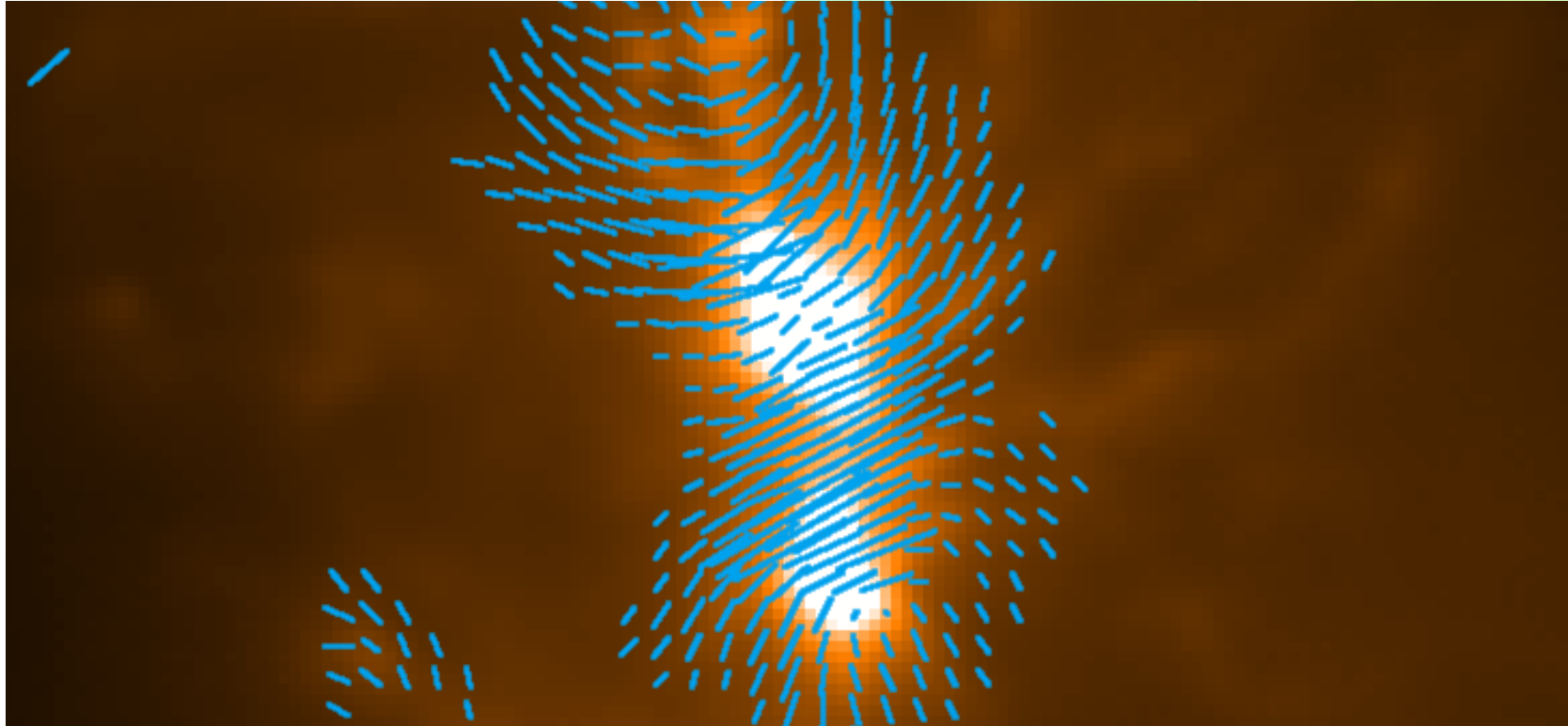


The Magnetic Field Strength and Energy Balance of OMC 1

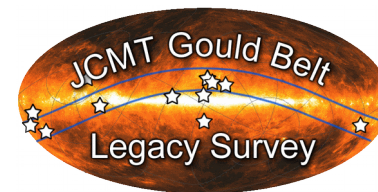
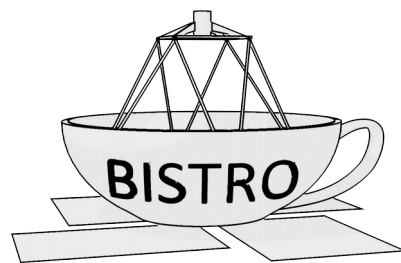


Credit: POL-2 Commissioning Team

Kate Pattle, University of Central Lancashire



JEREMIAH
HORROCKS
INSTITUTE




uclan
University of Central Lancashire

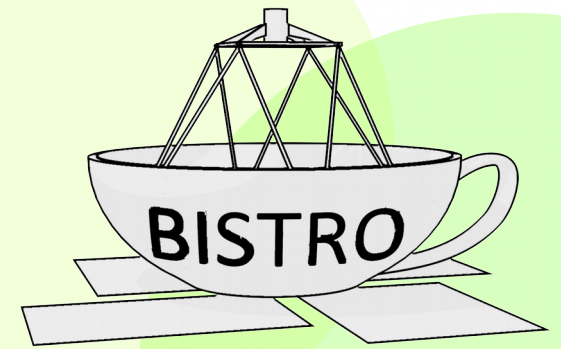
Acknowledgements:

BISTRO: Derek Ward-Thompson, Woojin Kwon, Tetsuo Hasegawa, Shih-Ping Lai, Keping Qiu, Pierre Bastien, Ray Furuya, Simon Coudé, Jongsoo Kim, Chang Won Lee, Andy Pon, Sarah Sadavoy, among many others

East Asian Observatory: David Berry, Jess Dempsey, Per Friberg, Sarah Graves, Harriet Parsons

Gould Belt Survey: James Di Francesco, Jenny Hatchell, Helen Kirk, among many others

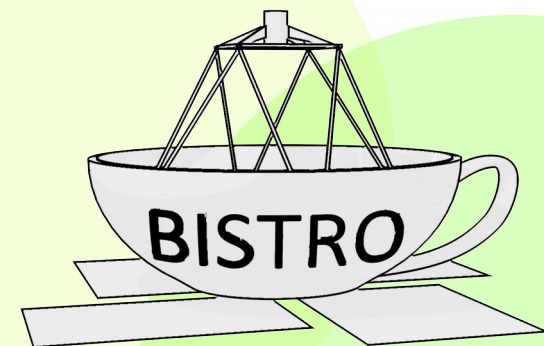
BISTRO: Overview



- We are a JCMT Large Program aimed at mapping the Gould Belt star-forming regions in polarised light
- >100 survey members across 6 partner regions and the East Asian Observatory
- P.I.s: Derek Ward-Thompson (UK), Tetsuo Hasegawa (Japan), Woojin Kwon (Korea), Shih-Ping Lai (Taiwan), Keping Qiu (China), Pierre Bastien (Canada)
- BISTRO-1 awarded 224 hours of observing time to map:
Ophiuchus, Orion A & B, Perseus, Serpens Main, Taurus L1495/B211, Auriga, IC5146
- BISTRO-2 (2017) awarded a further 224 hours to map:
More of Orion, more of Perseus, Serpens Aquila, M16, DR15, DR21, NGC 2264, NGC 6334, Mon R2, Rosette

Survey paper: **Ward-Thompson et al. 2017, ApJ 842 66**

BISTRO: Scientific Goals



- To map the magnetic field within cores and filaments, on scales of ~ 1000 - 5000 AU
- To determine magnetic field strengths in nearby molecular clouds using the Chandrasekhar-Fermi method (through synthesis with Gould Belt Survey HARP data)
- To investigate the relative importance of magnetic fields and turbulence to star formation
- To test the model of magnetic funnelling of material onto filaments (André et al. 2013; Palmeirim et al. 2013)
- To investigate the role of magnetic fields in shaping protostellar evolution
- To investigate the effect of magnetic fields on bipolar outflows from young protostars

POL-2: The Instrument



- A single-beam imaging polarimeter mounted on the SCUBA-2 camera on the JCMT (15m)
- Measures linear polarisation (Stokes Q & U)
- Takes data at $850\mu\text{m}$ (353 GHz) and $450\mu\text{m}$ (667 GHz) simultaneously. $850\mu\text{m}$ commissioned; $450\mu\text{m}$ commissioning ongoing
- 14" resolution at $850\mu\text{m}$, sensitive to spatial scales $\lesssim 5'$, mapping mode produces 12'-diameter maps with the option of mosaicing
- For details: Friberg et al. 2016, SPIE 9914 03

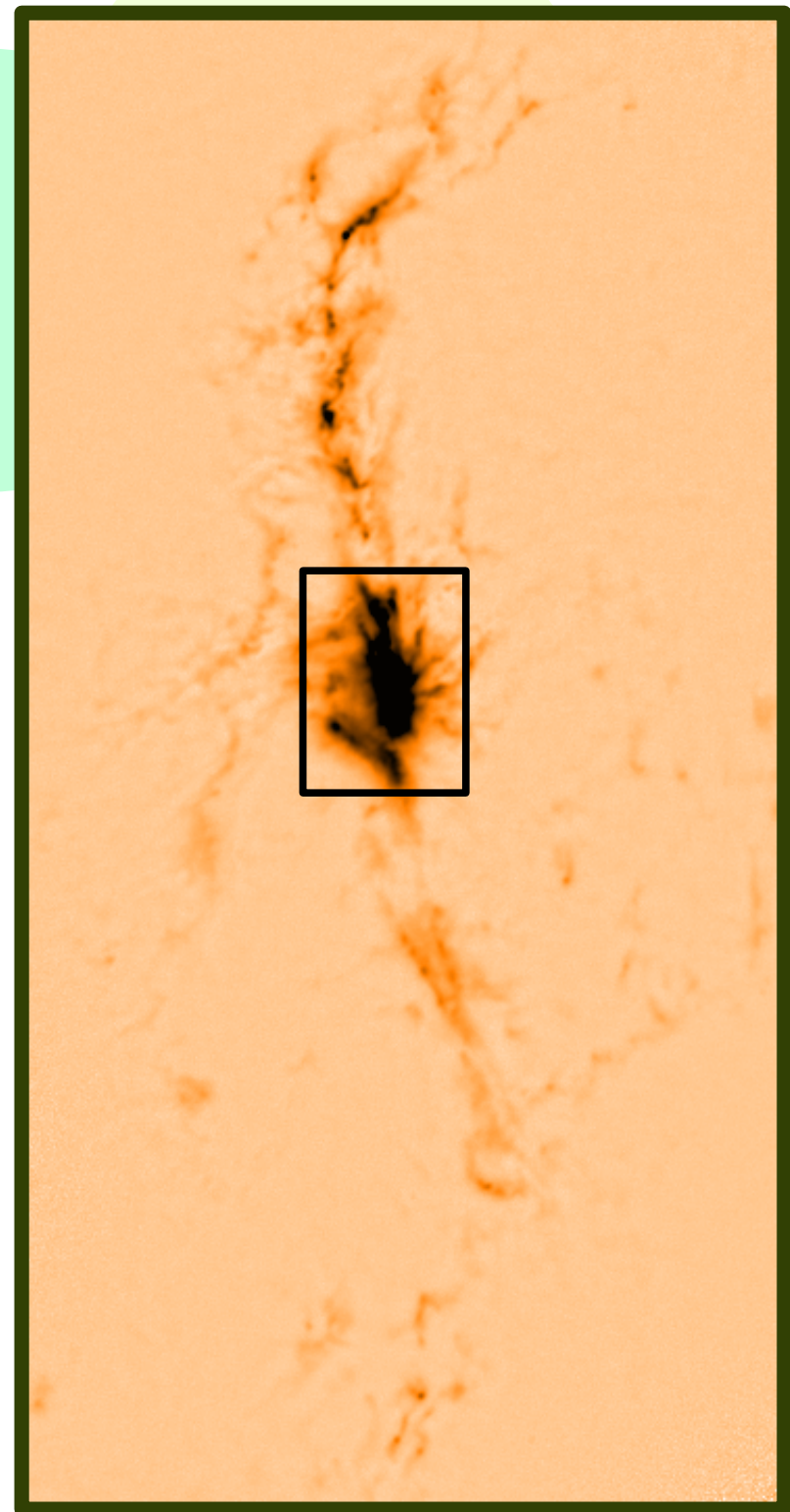
Orion A and OMC 1

The Orion Nebula is the nearest high-mass star-forming region.

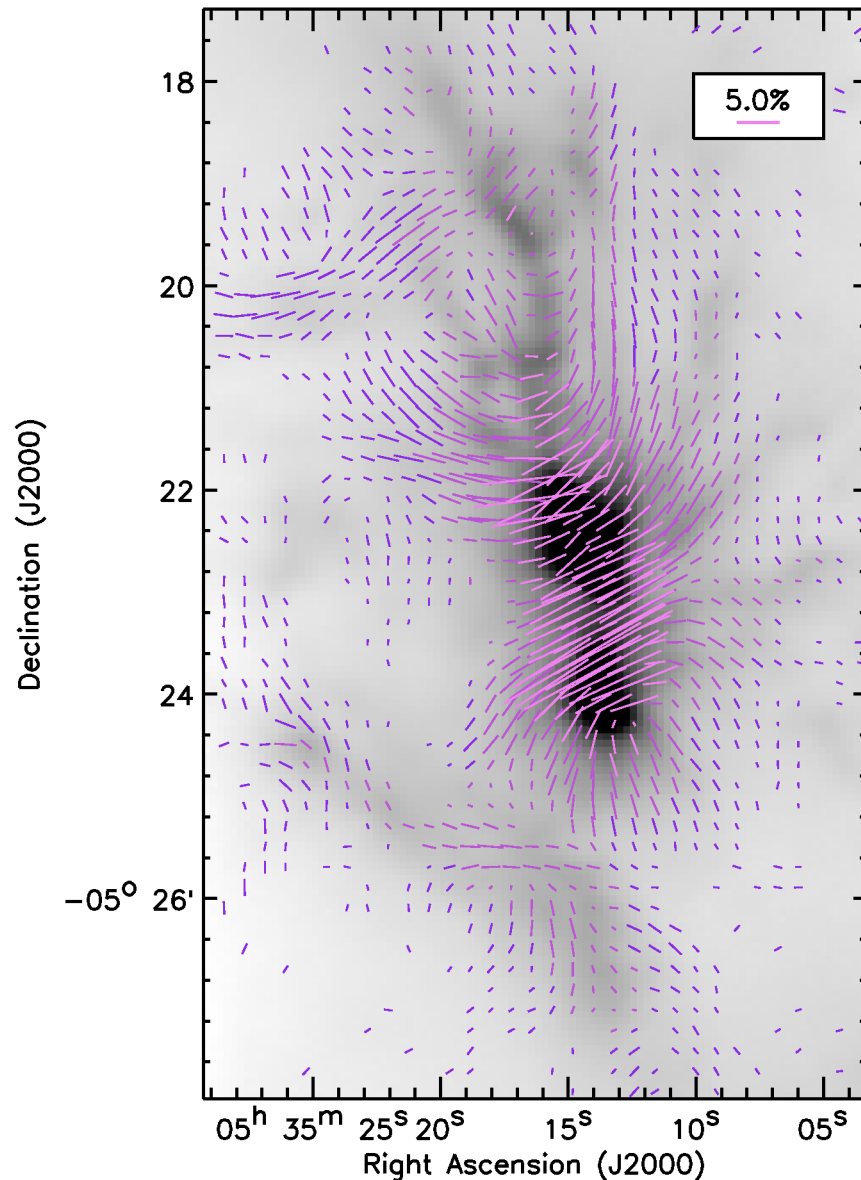
OMC 1 is a dense molecular cloud which is a site of ongoing high-mass star formation located in the centre of the Orion A “integral filament”, at a distance of 388 pc (Kounkel et al. 2017)

OMC 1 is located behind the Trapezium cluster, and bounded on one side by the Orion Bar PDR.

Image: CO-subtracted 850 μ m SCUBA-2 data;
JCMT GBS IR2 reduction



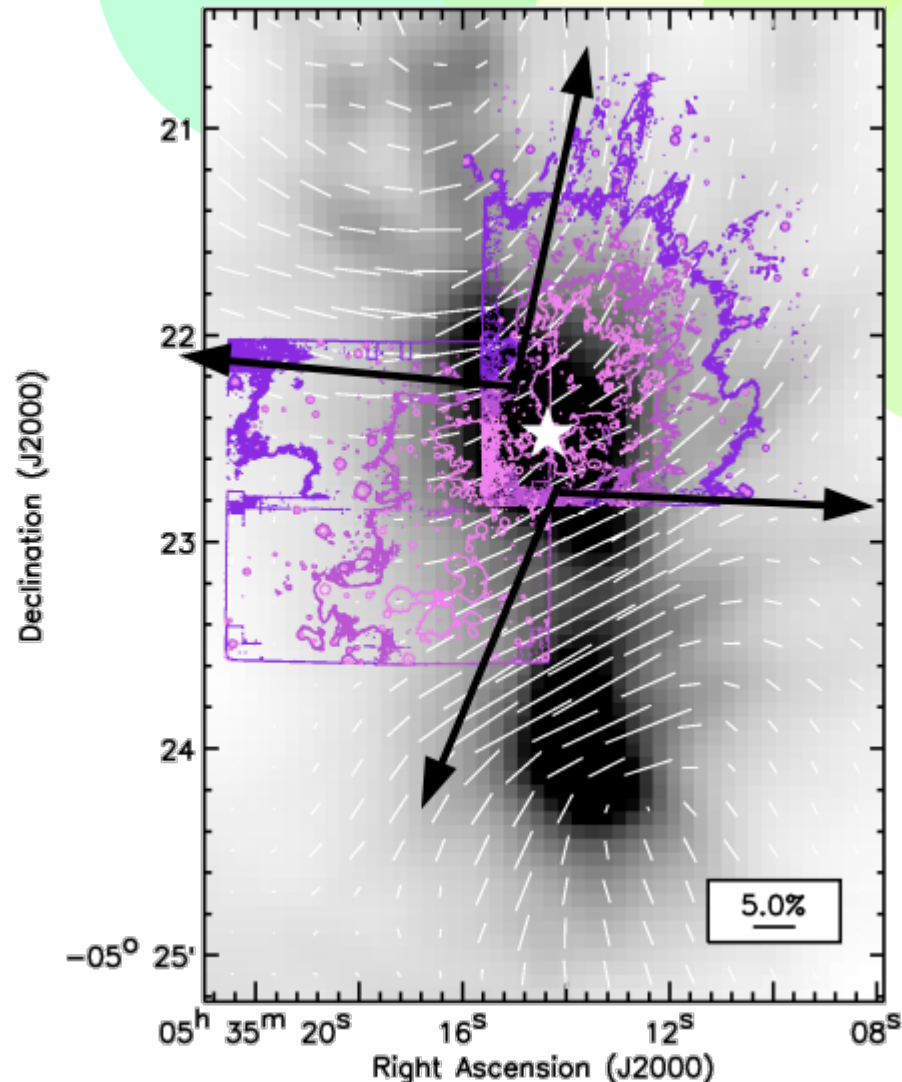
The magnetic field of OMC 1



- Observed in January 2016 as part of POL-2 commissioning and BISTRO science programmes
- $\sim 2\text{mJy/beam}$ RMS sensitivity on $12''$ pixels
- Vectors rotated to trace magnetic field
- Note ‘hourglass’ morphology (c.f. Schleuning 1998)

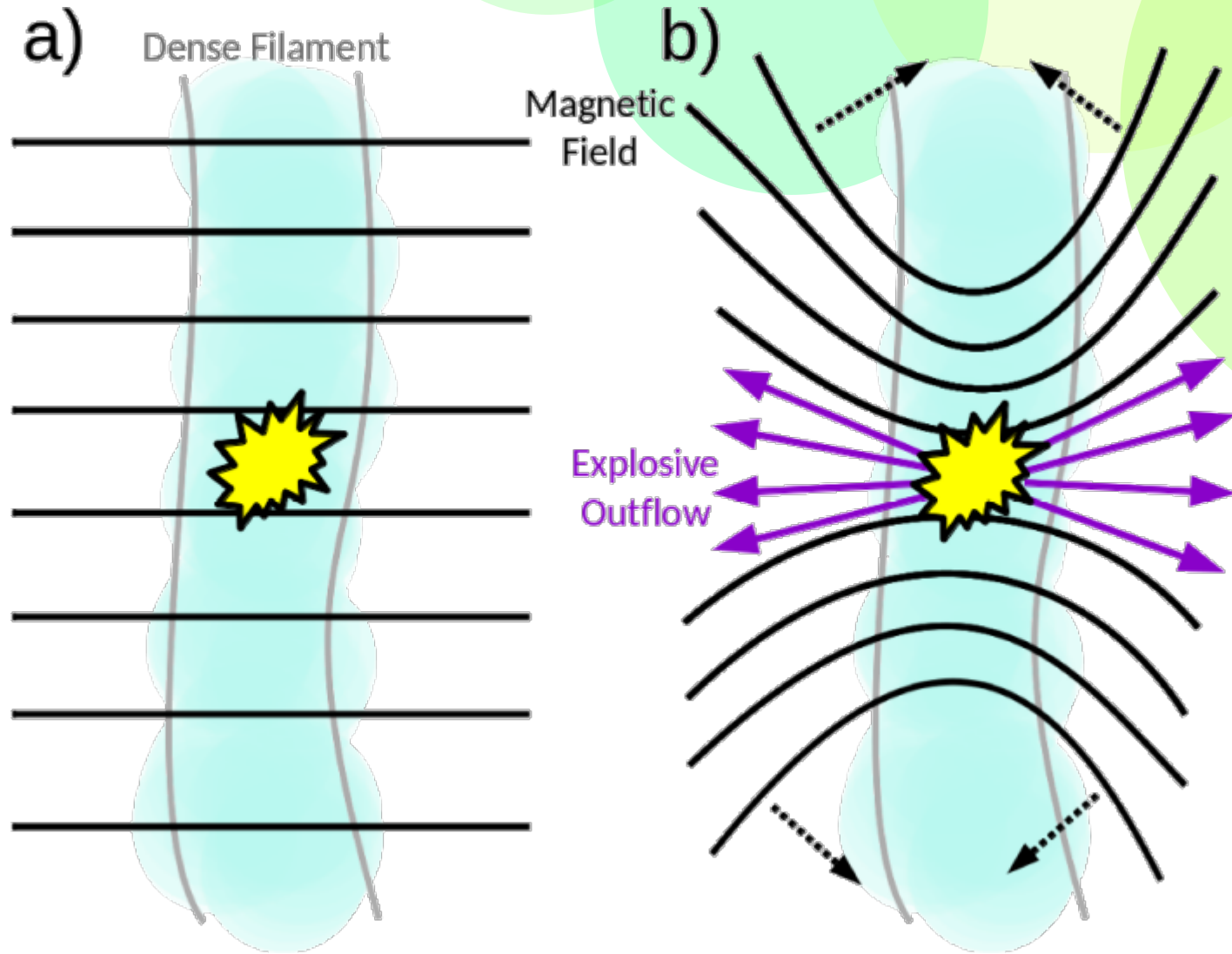
The BN/KL outflow

- a wide-angle explosive outflow with multiple ejecta (the “bullets of Orion”; Allen & Burton 1993)
- one of the most energetic outflows observed in a star-forming region: contains $\sim 4 \times 10^{47}$ erg of energy (Kwan & Scoville 1976)
- likely to have been formed by an encounter between Orion sources BN, n and I around 500 years ago (Gomez et al 2005; Bally & Zinnecker 2005)

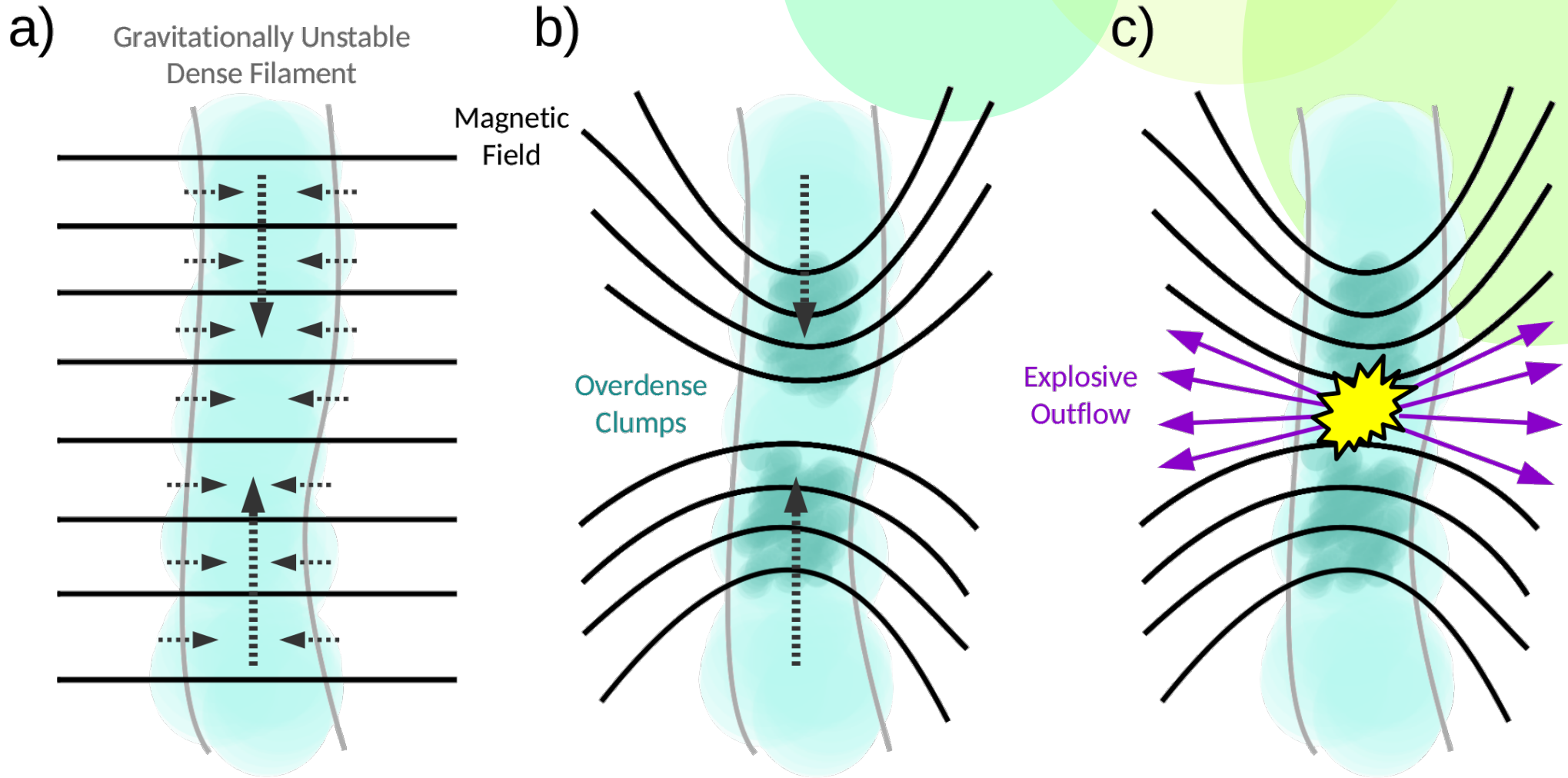


Contours:
H₂ emission
Bally et al.
2015

Hypothesis 1: Outflow shapes field

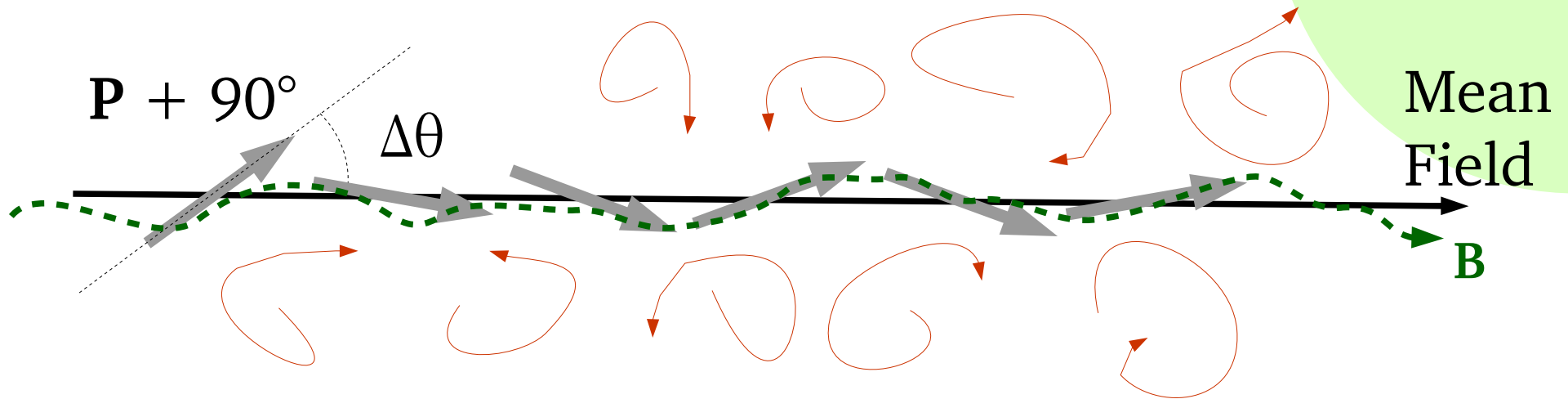


Hypothesis 2: Field shapes outflow



Chandrasekhar-Fermi Method

Assumes equipartition between non-thermal motions and the magnetic field: deviation in angle from the mean field direction is taken to be the result of distortion of the field by small-scale non-thermal motions (see Chandrasekhar & Fermi 1953).

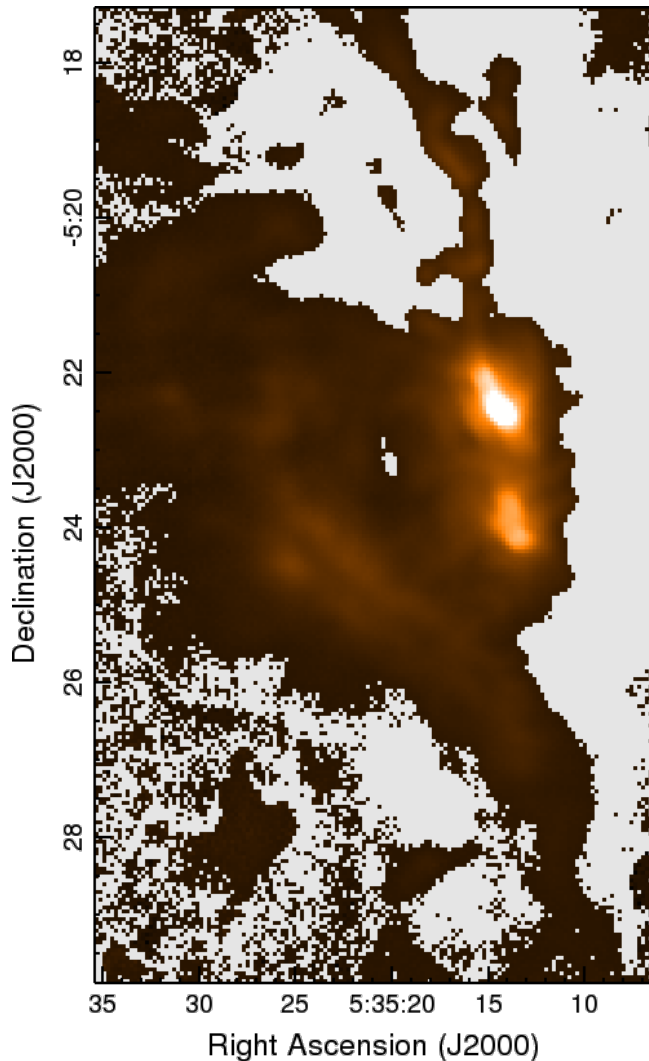


$$B_{\text{pos}} = Q \sqrt{4\pi\rho} \frac{\delta v}{\delta\theta} \approx 9.3 \sqrt{n(\text{H}_2)} \frac{\Delta v}{\langle\Delta\theta\rangle}$$

$$B_{\text{pos}} = \frac{\pi}{4} |\mathbf{B}| \quad (\text{c.f. Crutcher et al. 2004})$$

Volume Density:

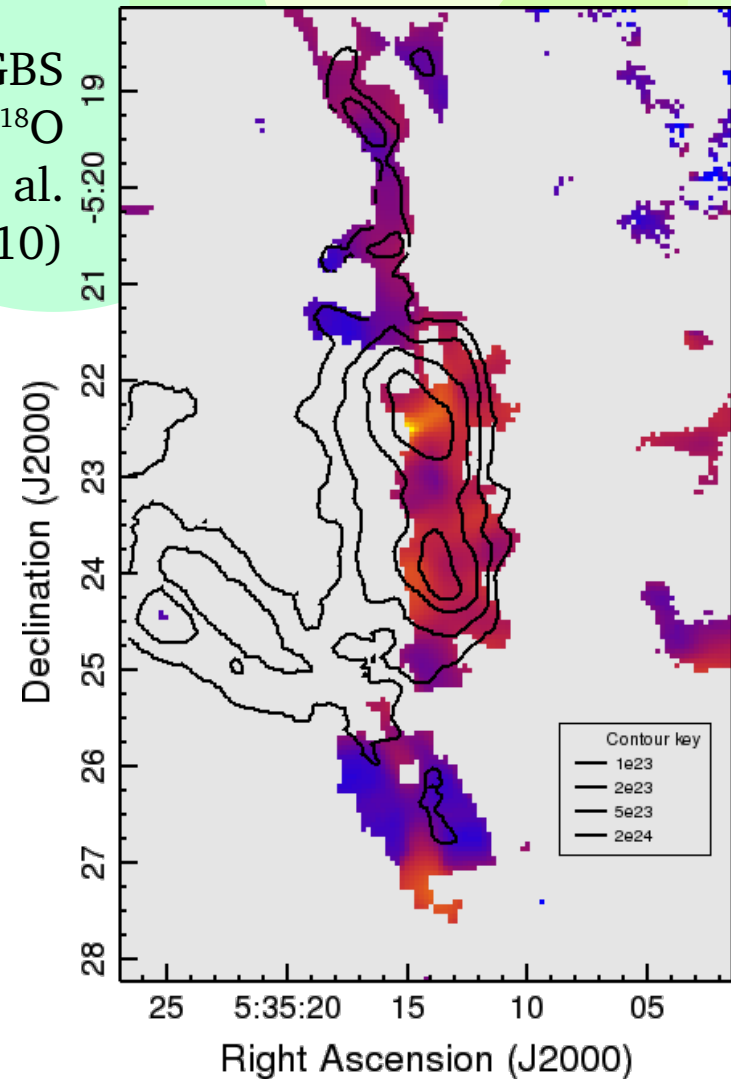
Velocity Dispersion:



JCMT GBS
SCUBA-2
450 μ m/850 μ m
Salji et al.
(2015a,b)

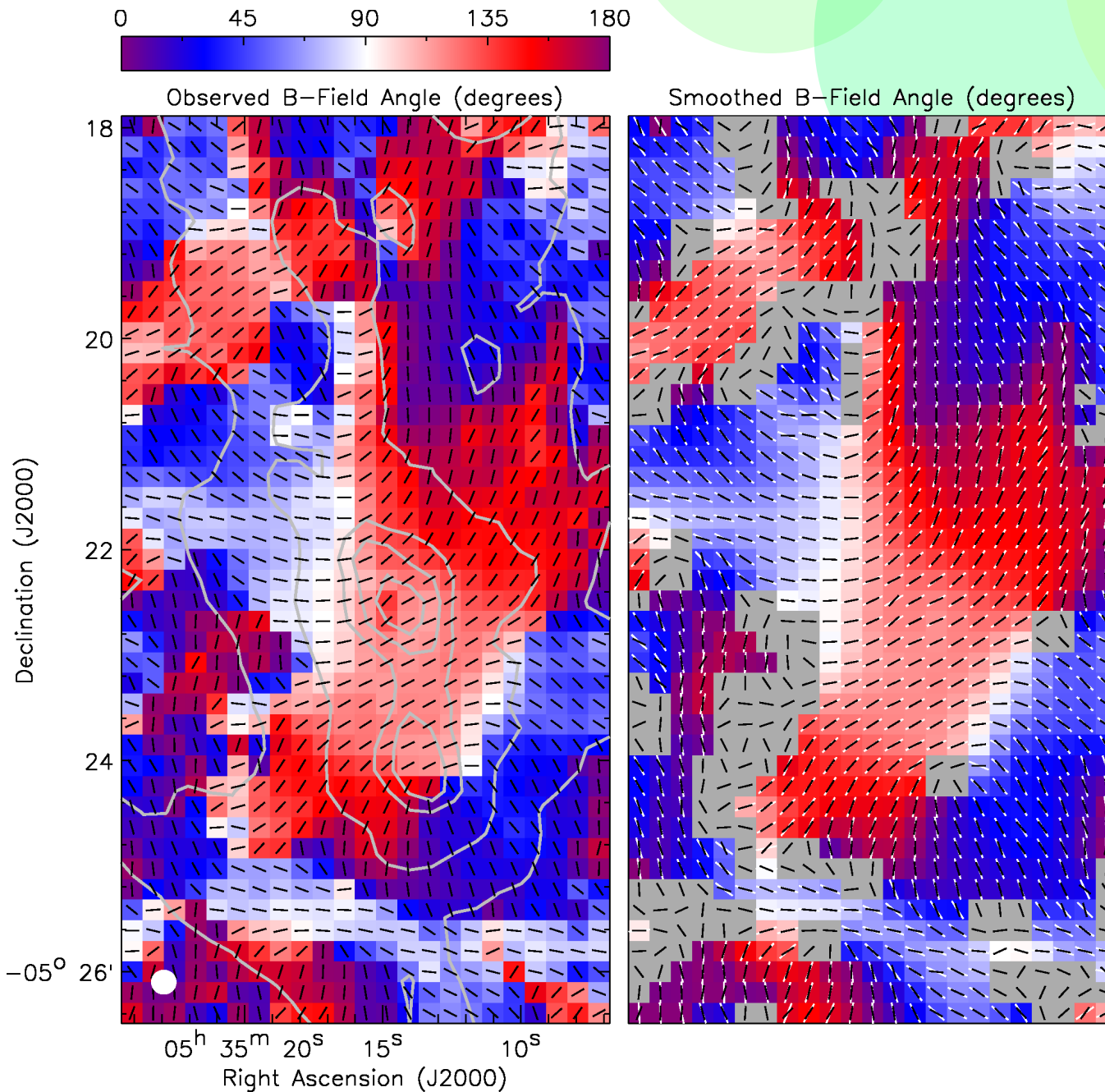
$$\begin{aligned} n(\text{H}_2) &= \frac{2N(\text{H}_2)}{\pi r} \\ &= (0.8 \pm 0.6) \times 10^6 \text{ cm}^{-3} \end{aligned}$$

JCMT GBS
HARP C¹⁸O
Buckle et al.
(2010)



Median 1D FWHM velocity dispersion in well-fitted pixels with S/N > 5: 3.19 km s⁻¹

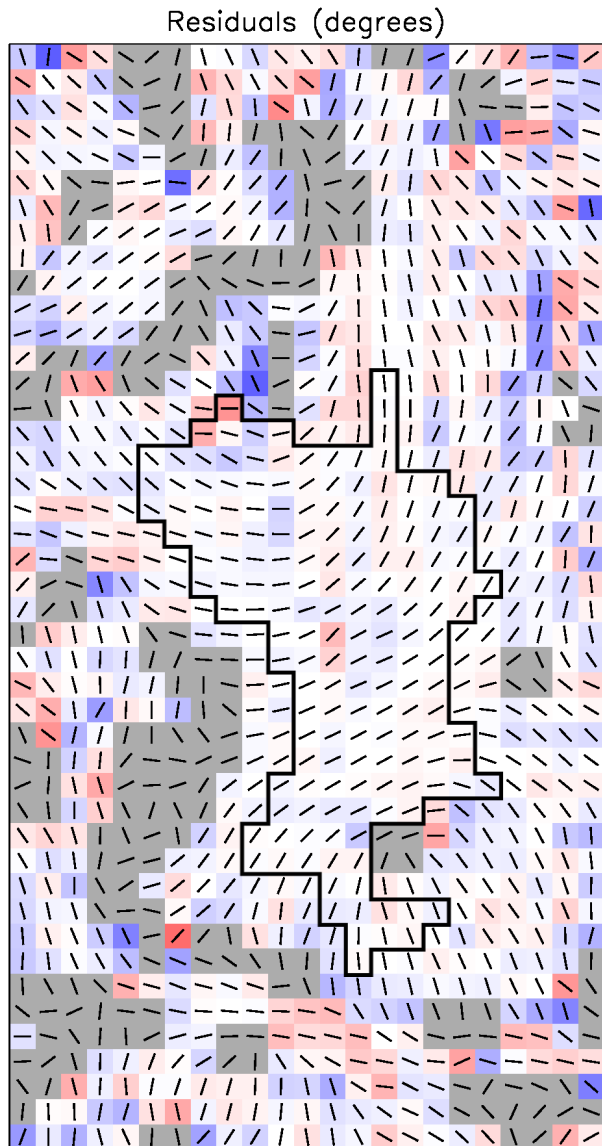
Deviation in angle: Unsharp masking approach



Mean field direction determined by smoothing with a 3x3 pixel box.

Pixels with $>90^\circ$ changes in angle inside the smoothing box excluded.

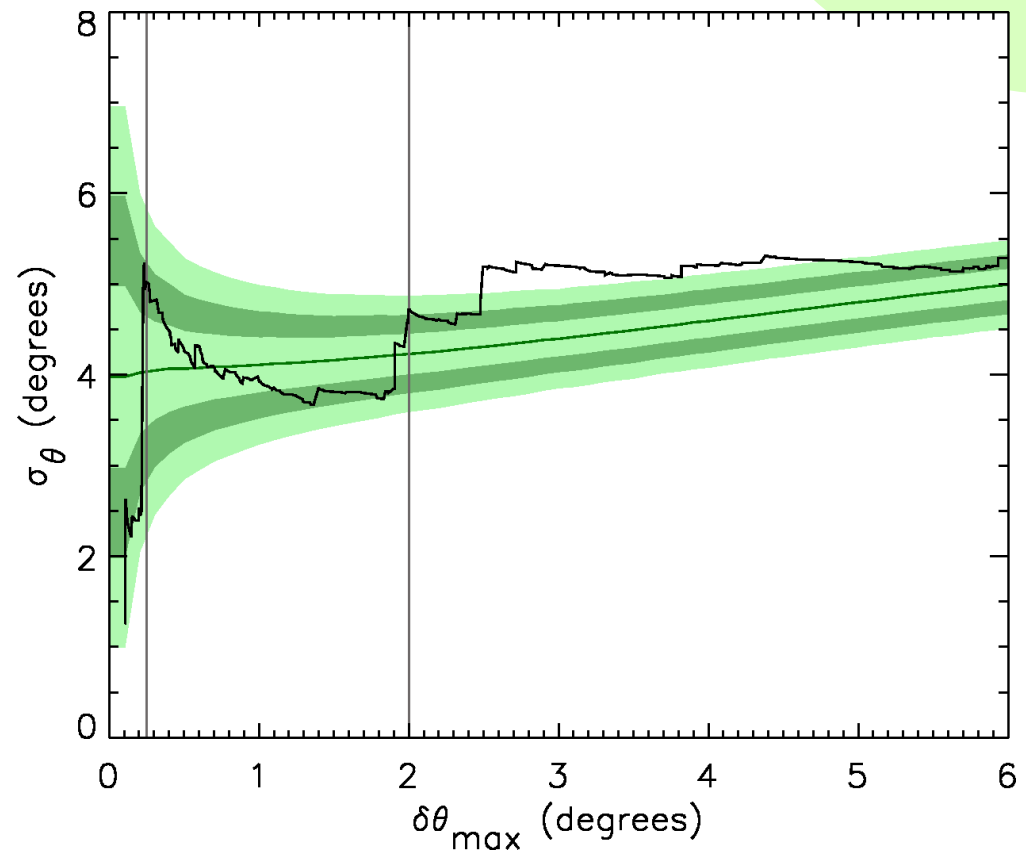
Deviation in angle: Unsharp masking approach



$$\Delta\theta = \theta_{obs} - \langle\theta\rangle$$

In pixels where $P/DP > 5$ and $\delta\theta_{max} < 2.0^\circ$:

$$\langle\sigma(\Delta\theta)\rangle: 4.0^\circ \pm 0.3^\circ$$



Magnetic field strength estimates

$$B_{\text{pos}} = Q \sqrt{4\pi\rho} \frac{\delta v}{\delta\theta} \approx 9.3 \sqrt{n(\text{H}_2)} \frac{\Delta v}{\langle\Delta\theta\rangle}$$

$$\Delta v = 3.12 \pm 0.73 \text{ km s}^{-1}$$

$$\langle\sigma(\Delta\theta)\rangle = 4.0^\circ \pm 0.3^\circ$$

$$n(\text{H}_2) \approx (0.8 \pm 0.6) \times 10^6 \text{ cm}^{-3}$$

Best estimate:

$$B_{\text{pos}} = 6.6 \pm 4.7 \text{ mG}$$

This value is consistent with previous estimates for OMC 1 (Hildebrand et al. 2009), and with values measured in other star-forming regions (Curran & Chrysostomou 2007)

Magnetic energy density

Using our measured magnetic field strength, we can estimate magnetic energy density in OMC 1:

$$U_B = \frac{|\mathbf{B}|^2}{2\mu_0}$$

If $B = 6.6 \text{ mG}$, then $U_B = 1.7 \times 10^{-7} \text{ J m}^{-3}$

How does this compare to the other sources of energy in OMC 1?

Gravitational potential energy density of the BN/KL – S system

From our column density map:

Mass of BN/KL: $1000 M_{\odot}$

Mass of S: $285 M_{\odot}$

Treating the system as a uniform cylinder:

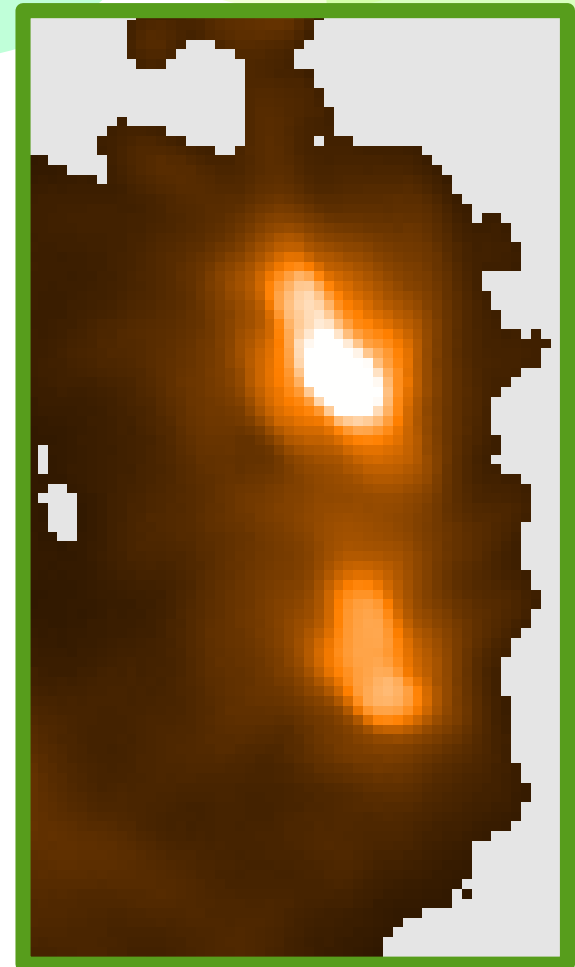
$$U_G = 1.9 \times 10^{-7} \text{ J m}^{-3}$$

Treating the system as a pair of point sources:

$$U_G = 0.5 \times 10^{-7} \text{ J m}^{-3}$$

Treating the system as a prolate spheroid:

$$U_G = 8.8 \times 10^{-7} \text{ J m}^{-3}$$



Outflow energy density

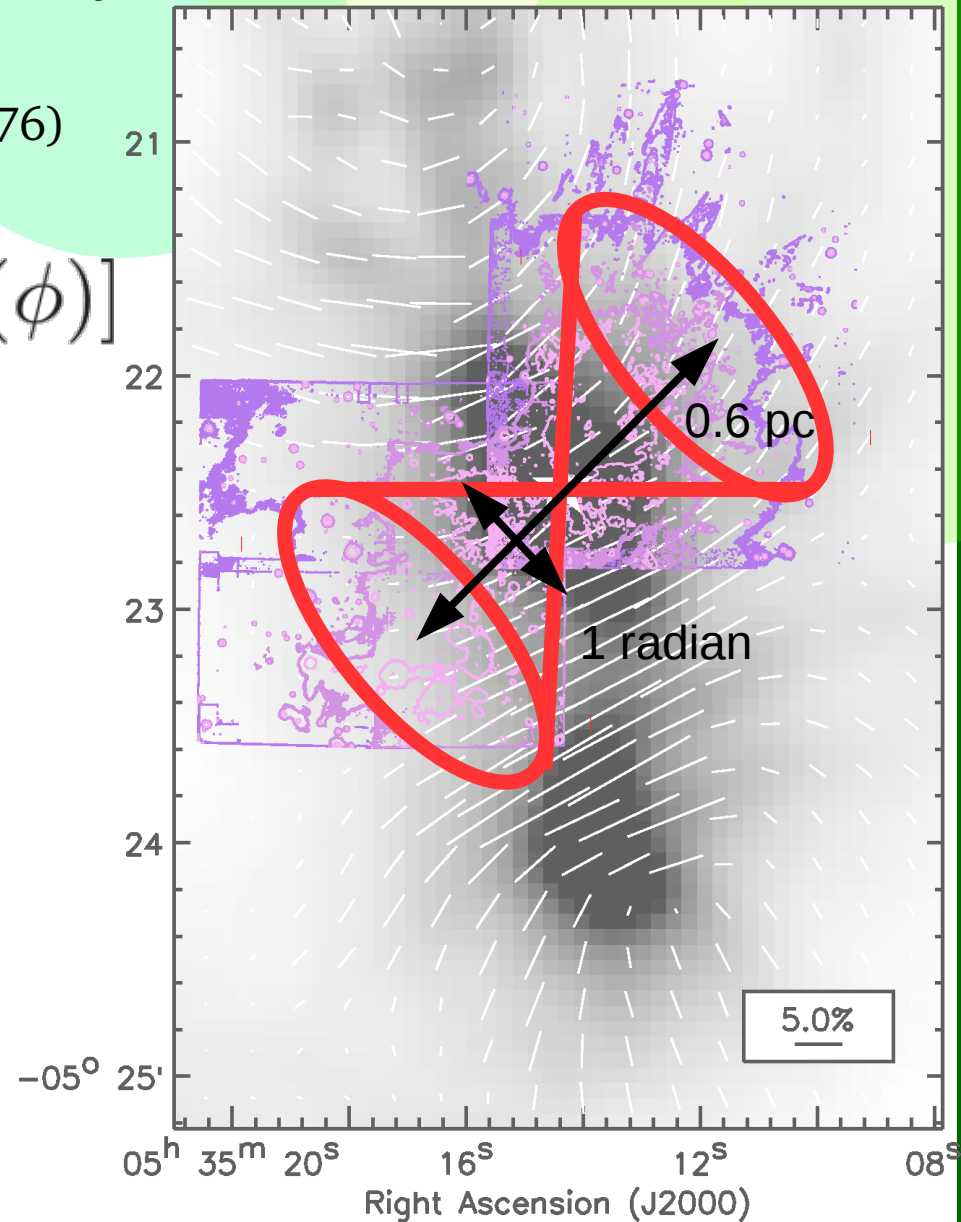
$$\sim 4 \times 10^{40} \text{ J} \quad (\text{Kwan \& Scoville 1976})$$

$$V_{\text{outflow}} = 2 \times \frac{2\pi r^3}{3} [1 - \cos(\phi)]$$

$$V_{\text{outflow}} = 2.7 \times 10^{47} \text{ m}^3$$

$$U_{\text{outflow}} \sim 1.5 \times 10^{-7} \text{ J m}^{-3}$$

However, knots are ballistic Herbig-Haro objects.
Total energy in knots $\sim 10^{37}$ J (Allen & Burton 1993). The large majority of the outflow energy is in the highly-collimated central outflow.



It seems that in OMC 1, if it doesn't have $\sim 10^{40}$ J of energy and an energy density of $\sim 10^{-7}$ Jm⁻³, it's not worth talking about:

$$U_B \sim 1.6 \times 10^{-7} \text{ J m}^{-3}$$

$$U_G \sim (0.5 - 8.8) \times 10^{-7} \text{ J m}^{-3}$$

$$U_{\text{outflow}} \sim 1.5 \times 10^{-7} \text{ J m}^{-3} \text{ (not uniformly distributed)}$$

So how can we tell which forces determine the magnetic field morphology?

Alfvén and ballistic velocities

$$c_A = \frac{B}{\sqrt{\mu_0 \rho}}$$

$$B = 6.4 \pm 2.1 \text{ mG},$$

$$c_A = 9.1 \pm 3.0 \text{ km s}^{-1}$$

Max. Alfvénic field deviation in 500 yr: $(4.6 \pm 1.5) \times 10^{-3} \text{ pc}$

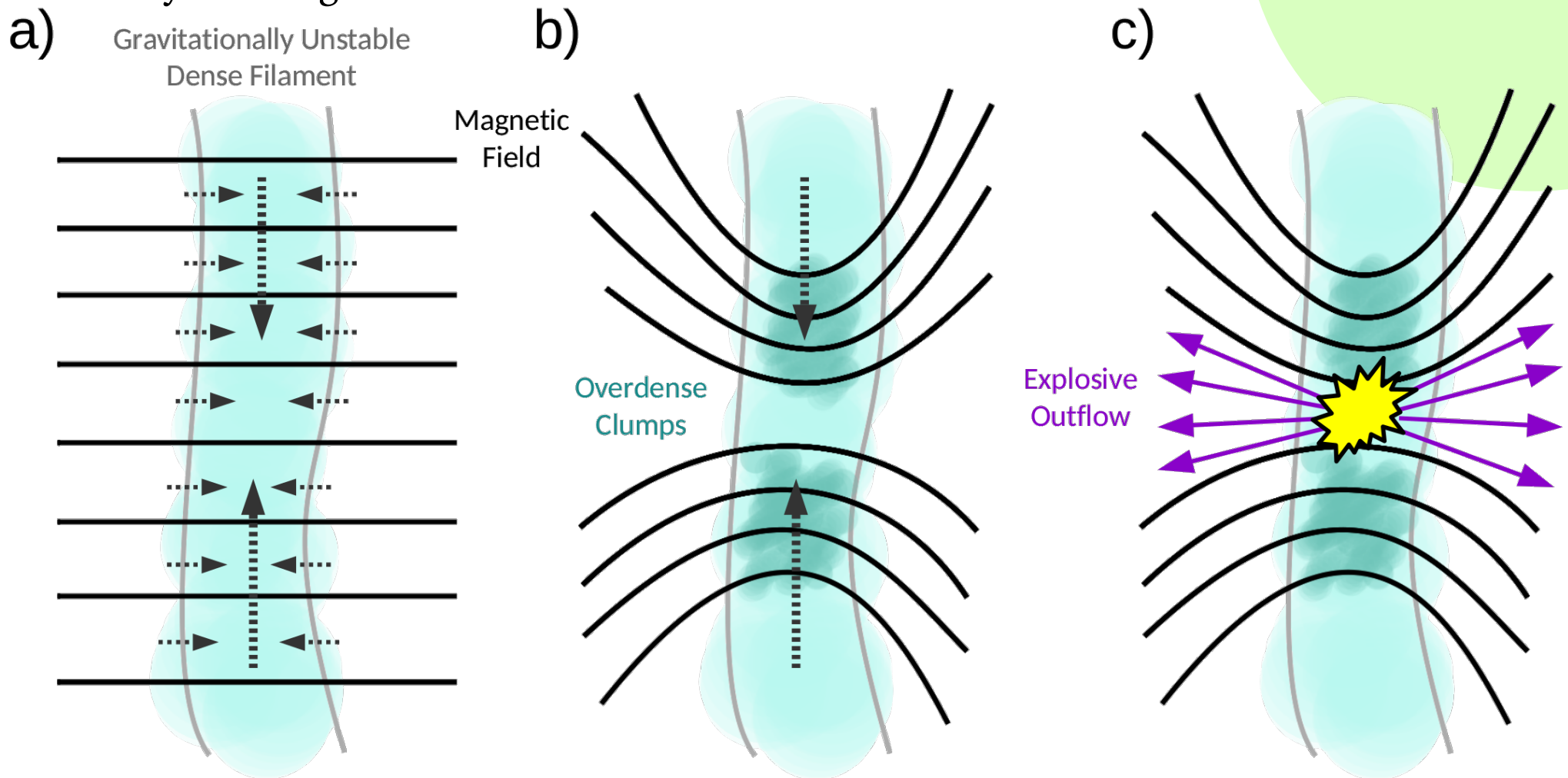
However, ejecta velocities are supersonic and super-Alfvénic:
Typical LOS ejecta velocity is $\sim 150 \text{ km/s}$ (Bally et al. 2017).

Max. distance travelled in 500 yr: $\sim 10^2 \text{ pc}$

Hence, the outflow **cannot** have caused the observed deviation in magnetic field lines in OMC 1 in the time since its formation.

Our results suggest that:

- The magnetic field strength and the gravitational force between BN/KL and S are in approximate balance
- The 'hourglass' magnetic field shape may have been produced by the gravitational interaction. The magnetic field may have been compressed until equilibrium was reached
- The orientation of the BN/KL outflow has, on large scales, been determined by the magnetic field

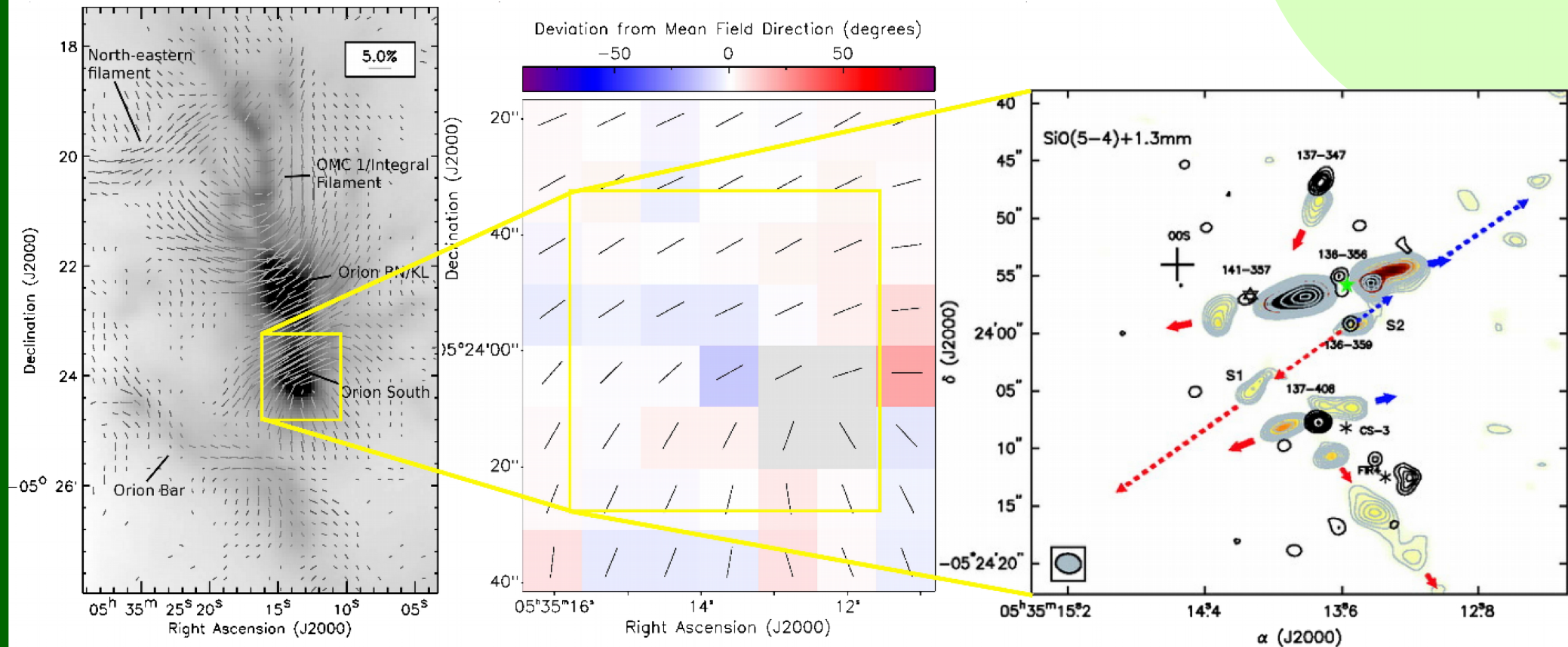


Finally: something about ALMA!

“Does magnetic field of the natal clump gas regulate outflows in a forming star cluster?”

PI: Ray Furuya, Co-Is: Pattle, Hasegawa et al.

- Band 7, 0.4-arcsec resolution dust continuum polarimetric imaging
- 4 outflow-driving sources in OMC1 South
- Grade B-ranked in Cycle 5

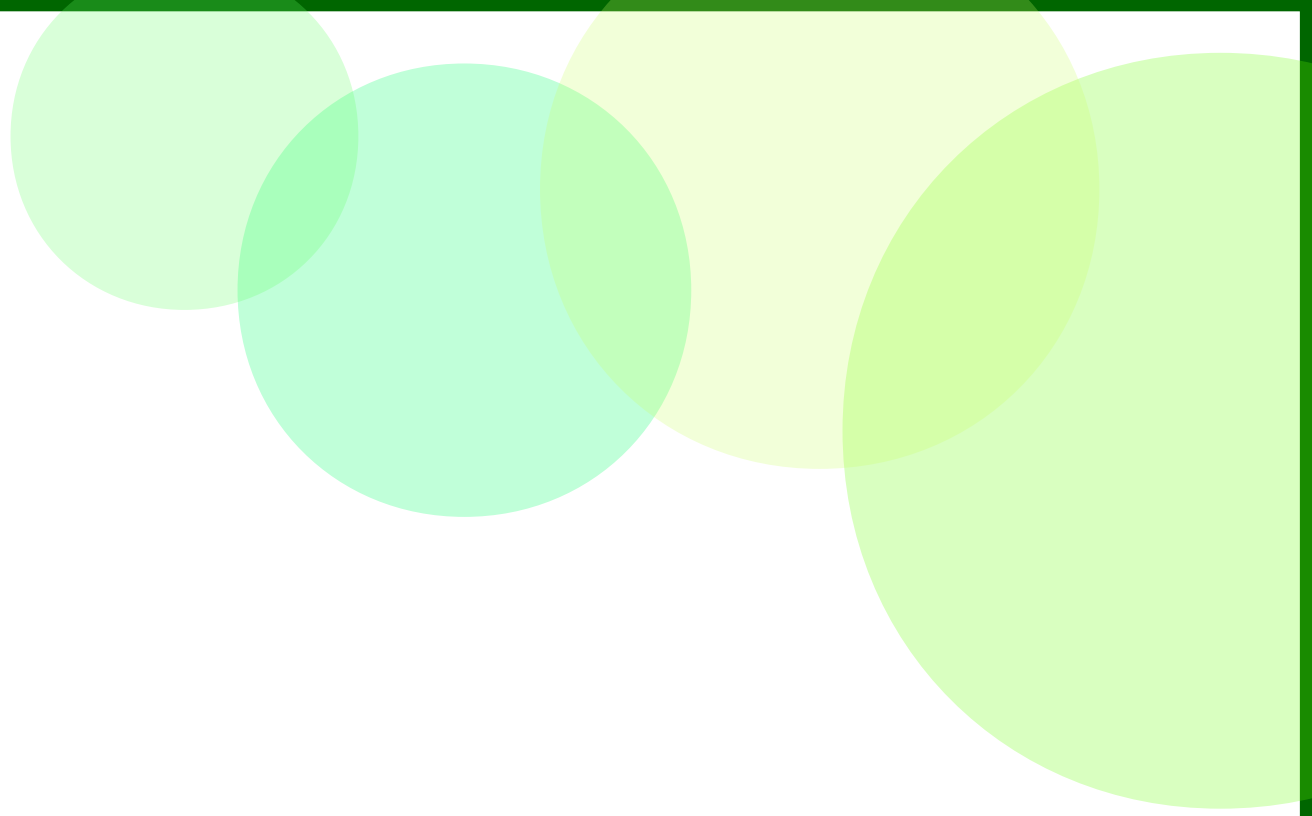


Conclusions:

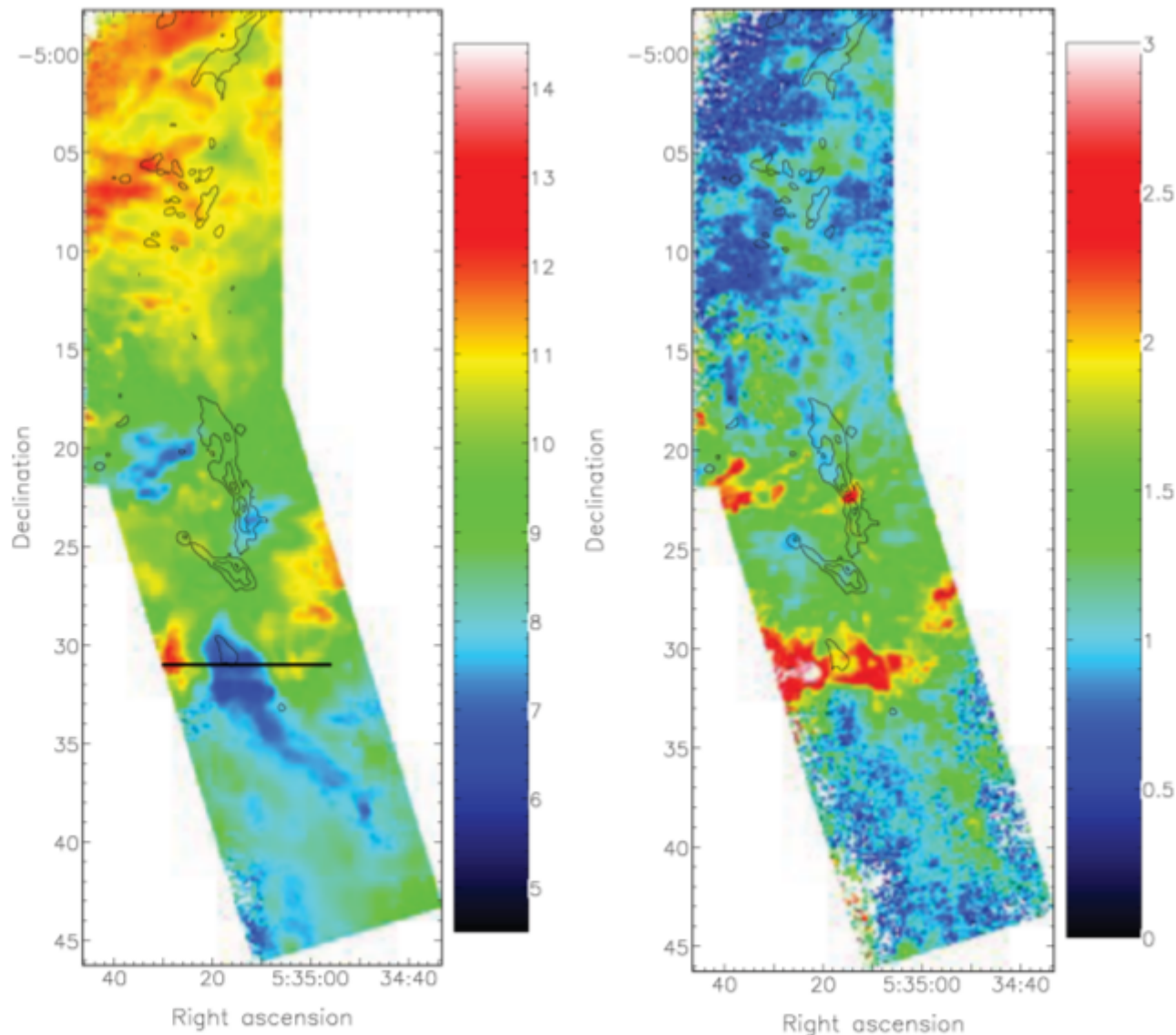
- We measure a magnetic field strength of 6.6 ± 4.7 mG in the OMC 1 region of Orion A, comparable to more distant high-mass star-forming regions
- We find that the magnetic, gravitational and outflow energy densities in OMC 1 are all $\sim 10^{-7} \text{ J m}^{-3}$
- The Alfvén velocity in OMC 1 is sufficiently small that the deviations in the magnetic field of OMC 1 could not have been created in the lifetime of the BN/KL outflow
- We suggest that the ‘hourglass’ morphology of the magnetic field in OMC 1 is caused by distortion of an initially-uniform magnetic field by the gravitational interaction of Orion BN/KL and AS
- We further suggest that the orientation of the large-scale BN/KL outflow is constrained by the orientation of the magnetic field.

•
For more detail: **Pattle et al. 2017, ApJ 846 122**

Thank you!



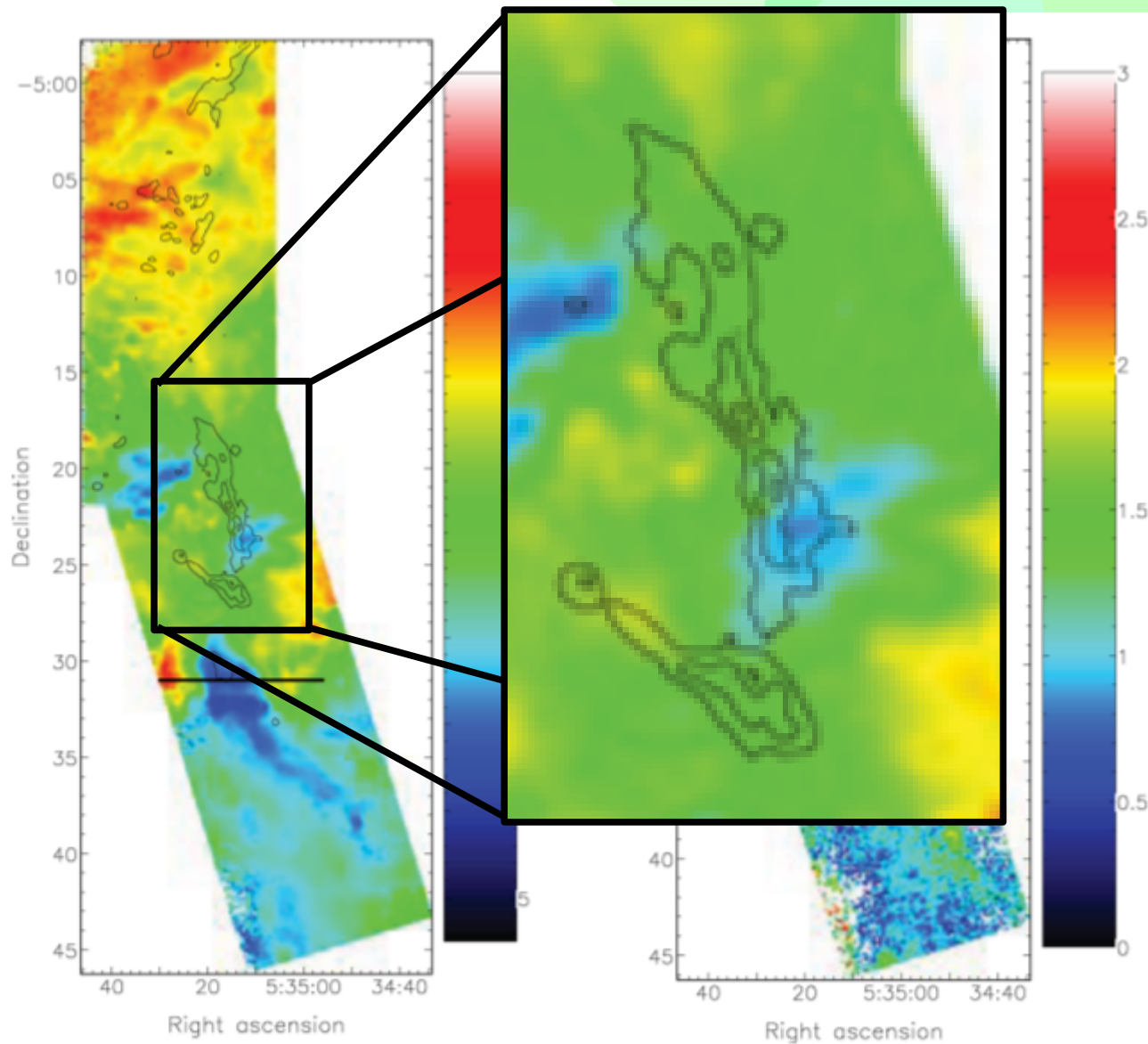
Velocity field in the OMC 1 region



HARP ^{13}CO
measurements;
Buckle et al.
2010

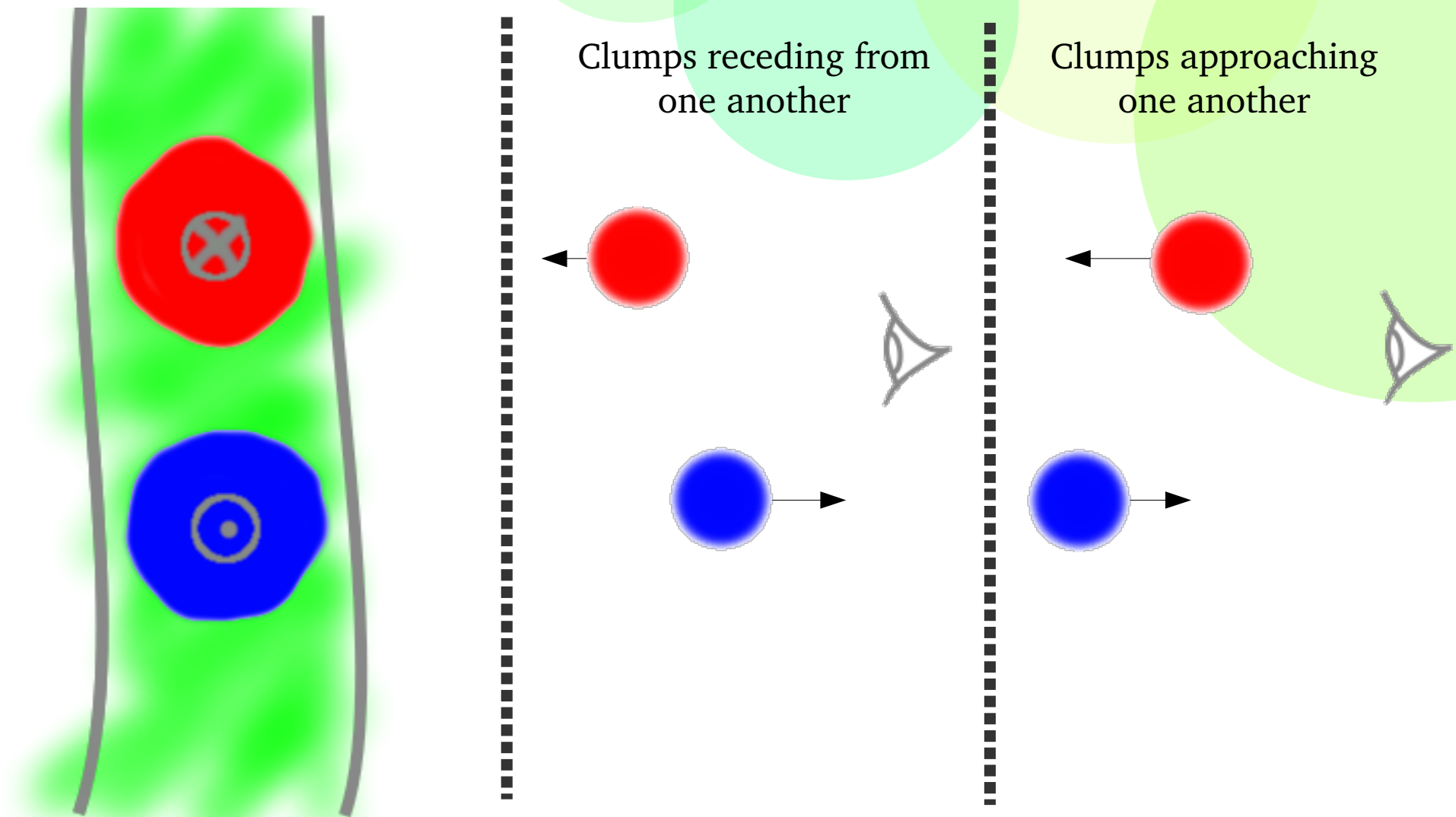
Figure 13. (a) ^{13}CO intensity weighted velocity map of Orion A, giving the velocity field in km s^{-1} . The black line marks the region between

Velocity field in the OMC 1 region



HARP ^{13}CO
measurements;
Buckle et al.
2010

There is more than one interpretation of this line-of-sight velocity...



Hence, we cannot exclude either hypothesis using velocity data alone.

GPE density: point-source model

From our column density map:

Mass of BN/KL: $1000 M_{\odot}$

Mass of AS: $285 M_{\odot}$

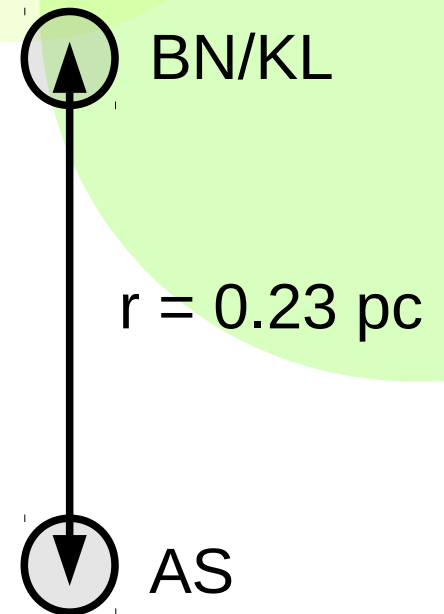
GPE of two point sources:
$$E_G = -\frac{GM_1 M_2}{r}$$

Plane-of-sky separation = 0.166 pc; for a conservative estimate of filament orientation, $r = 0.166 \times (2)^{0.5} \sim 0.23$ pc:

$$E_G = -1.0 \times 10^{40} \text{ J}$$

Assuming OMC 1 is a cylinder with height $0.321 \times (2)^{0.5}$ pc and diameter 0.141 pc:

$$U_G = -0.5 \times 10^{-7} \text{ J m}^{-3}$$



GPE density: prolate spheroid model

Prolate-spheroid model:

$$E_G = -\frac{8}{15}\pi^2 G \rho^2 a_1^4 a_3 \times \frac{1}{e} \ln \left(\frac{1+e}{1-e} \right)$$

(e.g. Binney & Tremaine 2008)

Assuming the BN/KL-AS system is a prolate spheroid with mass $1465 M_\odot$, semi-major axis $a_3 = 0.16$ pc and semi-minor axes $a_1 = 0.071$ pc:

$$E_G = -8.6 \times 10^{40} \text{ J}$$

$$U_G = -8.8 \times 10^{-7} \text{ J m}^{-3}$$

